Behavior of Reinforced Concrete Columns Subjected to Axial Load and Cyclic Lateral Load

Dr. Rafaa Mahmood Abbas
Lecturer
College of Engineering-University of Baghdad
E-mail: dr.rafaa@coeng.uobaghdad.edu.iq

Akram Ghulam Awazli
M.Sc
College of Engineering-University of Baghdad
E-mail: akgh1968@gmail.com

ABSTRACT

Columns subjected to pure axial load rarely exist in practice. Reinforced concrete columns are usually subjected to combination of axial and lateral actions and deformations, caused by spatially-complex loading patterns as during earthquakes causes lateral deflection that in turn affects the horizontal stiffness. In this study, a numerical model was developed in three-dimensional nonlinear finite element and then validated against experimental results reported in the literatures, to investigate the behavior of conventionally RC columns subjected to axial load and lateral reversal cyclic loading. To achieve this goal, numerical analysis was conducted by using finite element program **ABAQUS/Explicit**. The variables considered in this study were axial load index, concrete compressive strength, column aspect ratio, longitudinal and transverse reinforcement ratios.

According to numerical case studies, the results revealed that axial load index and longitudinal reinforcement ratio have the most impact on the column response. Also, increasing concrete compressive strength and reducing column aspect ratio resulted in increasing strength capacity of the column. Moreover, increasing lateral confinement by transverse reinforcement at the column ends increases the flexural strength of a flexure-controlled RC columns.

Key words: reinforced concrete columns, axial load, column failure, FEM, strength, cyclic load

سلوك الاعمدة الخرسانية المسلحة المعرضة لحمل محوري مع حمل جانبي ترددي

د.رافع محمود عباس
مدرس
كلية الهندسة- جامعة بغداد

أكرم غلام عوازلي
ماجستير
كلية الهندسة- جامعة بغداد

الخلاصة

ان الأعمدةُ المعرضة إلى حملِ محوري فقط قليلة جدا في الواقع العملي. حيث تتعرض الأعمدة الخرسانية المسلحة في الاغلب إلى تأثيرات تضم قوى محورية وجانبية والى تشوهاتِ، سببها أنماط تحميل معقدة في الفضاء (ثلاثية الابعاد) اثناء زلزال مثلا، مُسَبِّبة الازاحة الجانبية التي تُؤثِّرُ بدورها على الجسائة الأفقية. في هذه الدراسة، تم تطويرُ نموذجَ لا خطّي ثلاثي الأبعادِ من نماذجِ العناصرِ المحدودةِ ومن ثم التثَبَّتَ من صحة النتائج بالمقارنة مع النتائج التجريبية المثبتة بأدبيات البحوث، للتعرف على سلوكِ الاعمدة الخرسانية المسلحة الشائعة المعرضة لأحمال محورية وجانبية عكسية ترددية. ولتحقيق الهدف، اجري التحليل العددي باستخدام طريقة العناصر المحددة بواسطة برنامج ABAQUS/Explicit. المتغيرات التي تم دراستها في هذا البحث هي مؤشر الحمل المحوري، قوة انضغاط الخرسانة، ونسبة الارتفاع الى العرض، ونسبة التسليح الطولي والعرضي.

وفقا للدراسة العددية، اظهرت النتائج ان مؤشر الاحمال المحورية ونسبة التسليح الطولي لهما التأثير الاهم على استجابة العمود. كما ان زيادة قوة انضغاط الخرسانة اوتقليل نسبة الارتفاع الى العرض للاعمدة فأن ذلك يؤدي الى زيادة في قدرة مقاومة العمود. بالاضافة لذلك ان زيادة الحصر الجانبي بواسطة التسليح المستعرض في نهايات العمود يؤدي لزيادة مقاومة الانثناء للاعمدة التي يغلب عليها فشل الانثناء.

الكلمات الرئيسية: الاعمدة الخرسانية المسلحة, الاحمال المحورية, فشل الاعمدة, العناصر المحددة, المقاومة، الاحمال الدورية.

1. INTRODUCTION

Reinforced concrete frame buildings are the most common type of constructions. They are expected to show inelastic behavior and permanent residual drift angle or displacement under severe ground motion excitations. The stiffness, strength and ductility are the major characteristics of a structure to estimate its capacity. These characteristics are required to be analyzed properly and the factors affecting them must be studied in detail.

In frame structures, columns are the most critical structural elements as they provide stability by transmitting loads from super structure to foundation and furnish ductility. Due to their major contribution under seismic activity, they are the most vulnerable structural elements. Column's failure is the most vital as it may lead to additional failure and may result in complete collapse.
It is necessary to improve seismic performance for the RC columns by increasing their strength and ductility. Therefore, special care should be given to their behavior under load reversals.

2. FAILURE MODES OF RC COLUMNS

Failure modes describe the physical reason for the rupture of a structural element. **Fig.1** shows three probable different failure modes for RC columns; shear failure, flexural failure and flexural-shear failure, **Zhu, et al., 2007**. The main two causes for RC columns failure are lack of shear resistance which results in shear failure and insufficient deformation capacity which results in flexure failure and flexure-shear failure, **Acun,** and **Sucuoglu, 2010**.

Depending on intersecting point of the lateral load-deflection envelope curve and degradation of shear strength curve, modes of failure can be defined, **Yoshikawa,** and **Miyagi, 2001**. Failure modes may be shear failure; as shown in **Fig. 2A**, in which case the intersecting point is set before yielding of the main reinforcement and that happen when Plastic Shear Demand, V_p exceeded Nominal Shear Capacity, V_n resulting in a V_p / V_n ratio greater than 1.0. Flexural-shear failure occurs, as in **Fig. 2**Error! Reference source not found.**B**, in case the intersecting point is located after the main reinforcement yields. This failure mode happen when V_n is slightly higher than V_p resulting in a V_p / V_n ratio between 0.6 and 1.0. Flexure failure, as in **Fig. 2**Error! Reference source not found.**C**, occurs in case there is no intersecting point between the two curves which happen when V_n significantly exceeds V_p resulting in a V_p / V_n ratio less than 0.6.

According to the ACI 318, 2014, the nominal shear strength, Vn, is calculated as the summation of contributions from concrete, V_c, and the transverse reinforcement, V_s. happen

$$V_n = V_c + V_s \quad (1)$$

$$V_c = 0.17\,[1+p_u/(14*A_g)]\sqrt{f_c'}\,bd \quad (2)$$

Where; A_g is gross column area, P_u factored axial compression force, d is the effective depth of the column's cross-section, f_c' concrete compressive strength in (MPa). The shear reinforcement contribution is calculated as follows:

$$V_s = A_v f_y d / s \quad (3)$$

Where; A_v is the area of transverse reinforcement, f_y is the yield strength of the reinforcement, and s is the spacing of the shear reinforcement.

The plastic shear demand refers to the shear force at which flexural yielding occurs in the longitudinal reinforcement, forming plastic hinges in the maximum moment regions of the

specimen (which form at the bottom and top of columns subjected to double curvature). Therefore, the difference between the two strength envelopes plays a key role in predicting the failure mode of a given specimen.

3. EVALUATION OF COLUMN DISPLACEMENT CAPACITY

Elastic or linear analysis procedures are insufficient for the assessment of structure behavior because of the incapability to capture the modification of the structure response when inelastic action occurs, **Fig. 3A**. For structural assessment, the various nonlinear analytical procedures can be classified into two main sets: *Nonlinear dynamic analysis* (NDA) and *Nonlinear static analysis* (NSA), each one having its own shortcomings and strengths as in **Fig. 3B**.

Nonlinear dynamic analysis or time-history analysis is highly cost in time and money besides uncertain input for site-specific data and the effort for analysis and detailed modeling could not be warranted. Nonlinear static analysis as the pushover analysis is low costs in time and money and have become a desired analysis method in assessment of structural inelastic seismic behavior.

Monotonically increasing lateral loads at each time step during the analysis procedure to estimate seismic demands in pushover analyses. The modes of the load remain same, until a suggested displacement is reached or the structure collapse. The control method for doing the equivalent seismic loads can be displacement control method or force control method associated with the procedure that applied. The disadvantages of using the force control method are:

- At each step of the increment analysis, it is difficult to redefine the incremental force vectors after inelasticity develops in the structure
- The analysis may be terminate when the peak lateral load reached prior the ultimate displacement develop.

Hence, the displacement control method is suitable and is adopted in this study to investigate the lateral load-displacement response of reinforced concrete column and validating them against existing experimental test data. Finite element models have been developed by using ABAQUS (6.10) to discretize the column specimen (1D2) tested by **Acun, 2010,** which represent an isolated part of the columns of an existing building extracted from the inflection point as shown in **Fig. 4.** The displacement-time history imposed on the experimental test specimen, using the displacement control method, is shown in **Fig. 5**.

4. NUMERICAL INVESTIGATION PROCEDURE

The numerical analysis carried out in this study was achieved by the following steps;

- First, set up a three-dimensional FEM for the RC column, and pushover analysis was adopted for lateral load. Results from the pushover analysis taken as the baseline for the parametric study.
- Second, parametric study was performed on the baseline model, and results were compared for the global response.
- Discussion was carried out based on the influence of varying parameters made on the column ductility and lateral force demands. Carry out

5. FINITE ELEMENT MODELING

In this study the column specimen (1D2) tested by **Acun, 2010**, shown in **Fig. 4**, was modeled by the finite element method by using finite element code ABAQUS. The discretized column is modeled as a three-dimensional deformable solid body as shown in **Fig. 6**. Materials properties

and reinforcement details are given in **Table 1**, whereas the finite element types used for the working model are shown in **Table 2**.

5.1 Material Properties and Constitutive Relationships

Within finite element packages, reinforced concrete is considered a complex material to be modeled. Behavior of concrete in tension and compression should be certainly modeled with finite element in elastic and plastic range. Under tension behavior, the simulation should include tension stiffening, tension softening and local bond effects in RC elements. Under compression behavior, the model should include strain softening rules for inelastic behavior**.**

The concrete compression model requires linear elastic and inelastic material properties. The elastic limit is chosen as the stress corresponding to 0.3 f_c' for linear isotropic; (E_c) represents the modulus of elasticity of the concrete and (v_c) is Poisson's ratio of the concrete. The modulus of elasticity of concrete was based on the **ACI 318M-14** equation,

$$E_c = 4700\sqrt{f_c'} \qquad \text{(When } f_c' \text{ in MPa)} \tag{4}$$

The Poisson's ratio of concrete, ν_c, under uniaxial compressive stress varies from about 0.15 to 0.22 for normal strength. Hence, 0.2 was taken in the current study. The compression behavior curve for normal strength concrete in uniaxial compression is divided into three parts: one part in the elastic zone and two parts in the inelastic zone. The concrete compressive stress–strain relationship was defined using the following formulas.

For ascending branch, **Macgregor, 1992**:-

$$f_c = \varepsilon E_c \qquad \text{for} \qquad 0 \le \varepsilon \le \varepsilon_1 \tag{5}$$

$$f_c = \varepsilon E_c/(1 + \left(\frac{\varepsilon}{\varepsilon_\circ}\right)^2) \qquad \text{for} \qquad \varepsilon_1 \le \varepsilon \le \varepsilon_\circ \tag{6}$$

$$\text{And} \quad \varepsilon_1 = \frac{0.3\, f_c'}{E_c} \quad \text{(Hooke's law)} \tag{7}$$

$$\varepsilon_\circ = \frac{2f_c'}{E_c} \tag{8}$$

For the descending branch, **Hoshikuma, et al., 1997**:-

$$f_c = 0.85f_c' - E_{cd}(\varepsilon - \varepsilon_{cu}) \tag{9}$$

$$\text{And} \quad E_{cd} = \frac{0.85f_c'}{2\,\varepsilon_{cu}}$$

Where: - f_c = strength of normal concrete at any strain, ε
ε = strain associated with stress f_c .
ε_1 = strain corresponding to ($0.3f_c'$).
$\varepsilon_\circ$ = strain at peck point, at the ultimate compressive strength.
ε_{cu} = ultimate compressive strain.
E_{cd} = descending modulus of elasticity.

The ultimate compressive strain, ε_{cu} of the unconfined concrete is specified as 0.003 as recommended by the **ACI 318-14**.

In this study, the uniaxial tensile strength of concrete (f_t') as recommended by the **ACI 318M-14** for normal concrete ($f_t' = 0.62\sqrt{f_c'}$) is adopted; it has a corresponding strain equal to:

$$\varepsilon_t = f_t'/E_c \quad (10)$$

Therefore, the strain value of concrete strain at cracking for normal strength concrete is near to (0.000132) resulting from Eq. (10). It is reasonable to assume that the stress linearly reduces to (zero) at about 10 times the crack strain due to tension stiffening, **Abaqus Documentations, 2010**.

Tables 3 and 4 present concrete material characteristics using the above formulas for concrete compressive strength (f_c'=25.8 Mpa) that are used as input parameters for column (1D2) FE modeling, whereas **Fig.7** shows the plot for the stress-strain relationship for the concrete characteristics presented in these tables.

5.2 Element Selection and Input Values

5.2.1 Concrete

In numerical study, 8-node three dimensional hexahedral brick elements as C3D8R were selected to simulate the concrete (each node has three translational degrees of freedom) with reduced integration. Reduced integration elements are chosen in order to reduce computational time, which would be excessive in case of higher order elements. In addition, reduced integration is preferred in plasticity problems because elements do not exhibit volumetric locking when plastic flow occurs and incompressible material behavior takes place; it was preferred to use a denser mesh and low order elements.

Brick element able to model the behavior of nonlinear geometric and material of concrete and take into account the cracking in tension and crushing in compression by using **C**oncrete **D**amaged **P**lasticity model (CDP) to simulate the behavior of the concrete up to failure. **Fig. 8** shows a general view of the element. Tension and compression damage parameters used to simulate (CDP) model are listed in **Table 5**. Also, C3D8R element used to model steel plates that were placed on the top free end of the column.

5.2.2 Longitudinal and transverse reinforcement

In the analyses, the longitudinal and transverse reinforcement was modeled by using truss elements T3D2 as embedded throughout the column body, this type of element has two nodes. **Fig.9** shows a general view of the element and material properties for the steel reinforcement used in the column model are shown in the **Tables 6** and **7**.

5.3 Sequence of Load Application

For the numerical simulations involving axially loaded members under cyclic lateral load, the sequence of load application is in two separate analysis steps as follows:

a) Quasi-static step: The axial compressive load is applied during the natural period of the column.
b) Lateral dynamic step: It occurs after the column has achieved equilibrium**.**

5.4 Validation of the F.E. Models

Numerical modeling was developed to investigate the hysteretic response for the models under constant axial and lateral cyclic loads using nonlinear quasi-static analysis.

The verification case were confirmed by two widely accepted approaches:

- First**,** analyzed under monotonic loading behavior.
- Second, analyzed under reversed cyclic loading behavior.

By using pushover numerical analysis based on displacement control method and comparison with experimental results was made.

During the pushover analysis, the lateral displacement was increased step by step until the system reached the maximum displacement level attained in the experiment. Results for cyclic pushover analysis are presented in **Fig.10**.

Fig.10A, shows comparison for base shear-drift ratio response between experimental and numerical analysis for column specimen, while **Fig. 10B** shows the same comparison but for the lateral load-top displacement response. Results presented in these figures show good agreement between experimental cyclic response and that of the numerical finite element modeling.

The monotonic curve that corresponds to that of the half cyclic loading is illustrated in **Fig. 11** in comparison with the experimental and numerical cyclic base shear – drift ratio response for column. It is observed that peak values and limit of the response obtained by monotonic pushover analysis are in close agreement to those obtained by cyclic pushover analysis. Finally, **Fig. 12** shows a comparison of the stress distribution at the base of the column between analytical outcome and experimental testing for the column specimen.

6. PARAMETRIC STUDIES

Parametric study was conducted by using the finite element model. The study focused on the most important parameters that can affect lateral column response and the ultimate lateral load capacity was expressed in terms of:

- The applied axial load index, $\mathbf{P_{index}}$
- The longitudinal reinforcement ratio**,** $\boldsymbol{\rho}$
- The transverse reinforcement ratio**,** $\boldsymbol{\rho_s}$
- The Concrete compressive strength**,** $\mathbf{f'_c}$
- The Column aspect ratio, **L/ d**

In each analysis, only one variable is changed at a time, while all other parameters are kept constant (unchanged). The range of the parameters that are used in this study is summarized in **Table 8**.

6.1 Axial Load Index, P_{index}

Axial compression index, defined as the ratio of axial demand to axial capacity, is calculated from the following equation:

$$\text{Axial compression index } (P_{index}) = P/(A_g \cdot f'_c) \quad (11)$$

Practically, RC columns are commonly carry less than 20% of their pure axial load capacity (P_{index}<20%), **Sotoud,** and **Aboutaha, 2014**. The pushover analyses are performed to see the columns behavior under the effect of three levels of the axial load, with axial compression index values of 10%, 20%, and 40%, respectively. According to **Figs.13** and **14**, the results show that when increasing axial load index from 0.1 to 0.4, the peak base shear increased by 60% and the flexural strength is increased by about 75%.

It is interesting to mention that, after calculating V_n from Eq. (1), the V_p/V_n ratio for the reference column section ranged between (0.13 – 0.20) according to analytical results which confirm the flexure-controlled failure mode for the column.

6.2 Longitudinal Reinforcement Ratio, ρ

Practically, longitudinal reinforcement ratio for RC columns is 1% to 4%, **Sotoud,** and **Aboutaha, 2014**. Longitudinal reinforcement ratio is defined as follows:

$$\rho = (A_s / A_g). \quad (12)$$

The pushover analyses are carried out for three different (ρ) values (1%, 2.05%, and 3.2%) by using 8Ø14mm, 8Ø20mm, and 8Ø25mm rebars, respectively. The effects of varying the (ρ) on the lateral response of the column are shown in **Figs. 15** and **16.**

Results show that increasing the longitudinal reinforcement ratio from 1% to 3.2% for axial load index of 0.1, 0.2, and 0.4, respectively, causes an increase in the peak lateral force by (144%, 116% and 78%) and in the flexural strength by (129%, 105% and 67%), while the ultimate drift ratio decreased.

For the range of longitudinal reinforcement ratio that applied in the current study, it is observed that the V_p/V_n ratio for the column section ranged between (0.13–0.34) which confirms the flexure-controlled mode of failure for the adopted column configuration.

6.3 Transverse Reinforcement Ratio, ρ_s

Transverse reinforcement ratio, ρ_s is preferred to describe confinement and defined as the volume of transverse reinforcement divided by the volume of the concrete core per spacing length. Therefore the parameter, ρ_s is

$$\rho_s = A_v /(S*b) \quad (13)$$

To evaluate the effect of (ρ_s) on the capacity curves, three different ρ_s values are selected as (0.0041, 0.0061 and 0.0123) within the plastic hinging region. These values are achieved by varying ties spacing as follows:

1- For ρ_s= 0.0041 by using Ø8$_{mm}$ @ 105$_{mm.}$
2- For ρ_s= 0.0061 by using Ø8$_{mm}$ @ 70 $_{mm}$
3- For ρ_s= 0.0123 by using Ø8$_{mm}$ @ 35 $_{mm}$

As shown in **Figs. 17** and **18** the reduction of the ties spacing from 105 mm to 35 mm for axial load index of 0.1, 0.2, and 0.4 causes an increase in the peak lateral force by 6%, 10% and 13%, respectively. On the other hand, the flexural strength increases by 16% for the reduction in ties spacing from105 mm to 35 mm when axial load index equals 0.2.

6.4 Concrete Compressive Strength, f'_c

To investigate the influence of the concrete compression strength on the columns capacity, three pushover analyses were carried out for concrete strengths of 25MPa, 38 MPa and 50 MPa to account for this parameter in this study. All these values are within normal concrete strength range. The other parameters are almost the same as those of the reference column in each comparison.

Fig. 19, shows the effect of the concrete strength on base shear-drift ratio relationships when axial load index varied 0.1, 0.2 and 0.4 (for concrete strength 25 Mpa), respectively, and ρ =1%, ρ_s= 0.0061 are kept constant. Results indicated that the deformation capacities are not affected as long as the axial load index and (ρ_s) are kept constant; while the lateral load capacities are increased when concrete compressive strength is increased.

Increasing (f_c') from 25.8 to 50 Mpa for axial load index of 0.1, 0.2, and 0.4 (related to f_c'=25 Mpa) causes an increase in the peak lateral force by 19%, 14% and 12%, respectively, and the flexural strength increased by 20% for axial load index equals 0.2 as shown in **Fig. 20**.

6.5 Column Aspect Ratio, L/*d*

The aspect ratio so-called span to depth ratio, defined as the column or the story height-to-column depth ratio, determines the level of interaction between flexure and shear. **Wan et al., 2010** consider the aspect ratio as the key factor to describe the columns failure mode; when (L/*d* <2) then shear failure dominates and for (L/ *d* > 4) flexural governs failure mode. For (2 < L/*d* < 4), failure mode is uncertain here because both flexural and shear strength demands are equal, which is named as flexural-shear failure mode.

The selected column aspect ratios are 5.14, 3.5 and 2.8, while section details and material properties are the same for the reference column. The influence of aspect ratio on the peak lateral force is illustrated in **Fig. 21**. Results indicate that the peak lateral force increases with the decrease of the column aspect ratio.

According to the Results, the reduction of the (*L/ d*) ratio for axial load index of 0.1, 0.2, and 0.4 results in increase of the peak lateral force by 160%, 166% and 178%, respectively. The maximum V_p/V_n ratio for this model is (0.53) and the flexure-controlled failure mode is also dominate here.

7. CONCLUSION

Based on the analytical investigation reported in this study, the following conclusions are presented:-

1. Results indicated that the three dimensional finite element model used in this study was able to capture the major performance characteristics of reinforced concrete columns under combined axial and cyclic lateral loading by using ABAQUS/Explicit with the associated elements and material behavior models. In addition, it was shown that the suggested model was capable of predicting the peak lateral load with reasonable accuracy.
2. With an increase of the axial compression index, the longitudinal reinforcement ratio, and concrete compressive strength the peak lateral force increased, whereas the peak lateral force decreased with the increase of the aspect ratio.
3. An increase in the axial load index from 10% up to 40% causes an increase of about 60% in the peak lateral load and 75% in maximum flexural capacity of the columns. While increasing longitudinal reinforcement ratio from 1% up to 3.2% causes an increase of about 144% and 129% in the lateral load and flexural capacity of the columns, respectively, for axial load index 0.1.
4. Increasing lateral confinement of concrete by transverse reinforcement at the column ends has a considerable effect on the flexural strength of the column. Bending capacity of the column increased by 16% when transverse reinforcement ratio increased three times by reducing ties spacing.
5. Presence of axial compressive load improved the shear resistance capacity of the section, and for most cases, increased the ultimate moment of the section.
6. Finally, it can be concluded that with sufficient lateral confinement by transverse reinforcement, reinforced concrete columns can resist combination of axial and cyclically lateral loading efficiently, such as seismic loading, especially for flexural dominated failure to assure ductility and maintain seismic performance.

REFERENCES

- Abaqus Documentations 6.10, 2010, *Abaqus Documentation*, Dassault Systèmes Simulia Corporation, Rhode Island.
- ACI 318-14, 2014, *Building Code Requirements for Structural Concrete*, ACI Committee 318, American Concrete Institute, Farmington Hills, MI, USA.
- Acun, B., and Sucuoglu, H., 2010, *The Effect of Displacement History on the Performance of Concrete Columns in Flexure*, Advances in Performance-Based Earthquake Engineering, Vol. 13, No. 3, PP. 373-382.
- Acun, B., 2010, *Energy Based Seismic Performance Assessment of Reinforced Concrete Columns.*, Ph.D. Thesis, The Graduate School of Natural and Applied Sciences, Middle East Technical University.
- Adolfo M., 2006, *Degrading Slope for Post-Peak Response of RC Columns Subjected to Load Reversals*, Proceedings, the second NEES/E-Defense Workshop on Collapse Simulation of Reinforced Concrete Building Structures, October 31-November 1, E-Defense, Kobe, Japan, PP. 267-280.
- Hoshikuma, J., Kawashima, K., Nagaya, K., and Taylor, A. W., 1997, *Stress-Strain Model for Confined Reinforced Concrete in Bridge Piers*, Journal of Structural Engineering, ASCE, Vol. 123, No. 5, PP. 624-633.
- Macgregor, J. G., 1992, *Reinforced Concrete Mechanics and Design*, Prentice-Hall, Inc., Englewood Cliffs, NJ.
- Sotoud, S., and Aboutaha, R. S., 2014, *Performance of RC Bridge Columns Subjected to Lateral Loading*, Istanbul Bridge Conference. Proceedings of the Istanbul Bridge Conference, 2014, Istanbul, Turkey.
- Wan, H. Han, X., and Ji, J., 2010, *Analyses of Reinforced Concrete Columns by Performance-Based Design Method*, Journal of Central South University, Vol. 41, No. 4, PP. 1584-1589.
- Yoshikawa, H., and Miyagi, T., 2001, Ductility *and Failure Modes of Single Reinforced Concrete Columns*, American Society of Civil Engineers.
- Zhu, L., Elwood, K. J., and Haukaas, T., 2007, *Classification and Seismic Safety Evaluation of Existing Reinforced Concrete Columns*, Journal of Structural *Engineering*, 2007, Vol. **133** No. 9, PP. 1316-1130.

NOMENCLATURE

A_g = cross-sectional area, mm^2.
A_s = is the area of longitudinal reinforcement, mm^2.
A_v = total transverse reinforcement area within spacing, mm^2.
b = width of column section, mm.
d = column depth, mm.
E_c = modulus of elasticity of concrete
L = height of column section, mm.
P = applied axial load, N.
S = spacing of transverse reinforcement, mm.
V_c = shear force carried by concrete, N.
V_{max} = maximum of applied horizontal force, N.

V_n = nominal shear strength of columns
V_u = theoretical flexural strength of columns, N.
f_c' = compressive strength of concrete, Mpa.
Ø = diameter of longitudinal bars, mm.
ρ = longitudinal reinforcement ratio, dimensionless.
ρ_s = transverse reinforcement ratio, dimensionless.
ε_c = strain of concrete, dimensionless.
ε_{cu} = ultimate rupture strain of plain concrete, dimensionless.
f_u = ultimate strength of steel, Mpa.
f_y = yield stress of steel, Mpa.
δ_u = ultimate drift ratio, dimensionless.
δ_y = yielding drift ratio, dimensionless.
Δ_u = ultimate displacement at 80% of the horizontal loading position, mm.
Δ_y = yielding displacement at 65% of the horizontal loading position, mm.
u_Δ = displacement ductility factor, dimensionless.

Table 1. Material properties and reinforcement for column test specimen, Acun, 2010.

Specimen	Concrete	Longitudinal reinforcement			Transverse reinforcement		
	Compressive Strength f_c' (MPa)	Yield Strength f_y (MPa)	Ultimate Strength f_u (MPa)	Reinforcement Ratio ρ	Yield Strength f_y (MPa)	Ultimate Strength f_u (MPa)	Reinforcement Ratio ρ_s
1D2	25.8	454	604	0.01	469	685	0.0061

Table 2. Element types for working models.

Element No.	ABAQUS	Material Type
1	C3D8R	Concrete of column
2	C3D8R	Steel Plates (top)
3	T3D2	Longitudinal steel reinforcement
4	T3D2	Stirrups (Φ8 mm)

Table 3. Concrete characteristics definition input for column model.

Material characteristics	Property	Parameter	1D2 specimen
Density	-	Mass Density	2400 kg/m^3*
Elastic	Isotropic	Young's Modulus	23.873 GPa
		Poisson's Ratio	0.2*

* Assumed values

Table 4. Concrete material behavior definition input for column model

Concrete Damaged Plasticity				
Dilation Angle		Tensile Behavior	f_t (MPa)	ε_t
36*			3.15	3.15
Eccentricity			0	0.00132
0.1*		Compressive Behavior	f_c (MPa)	ε_c
f_{b0}/f_{c0}			3	0
1.16*			7.02	0.0003
Kc			11.33	0.0005
0.667*			16.8	0.0008
Viscosity Parameter			19.66	0.001
0*			24.17	0.0015
			25.8	0.00216
			21.93	0.003
			18.275	0.004
			14.62	0.005

***** Assumed values

Table 5. Damage model (CDP) parameters

Damage parameters			
Compression		**Tension**	
Damage Parameter	**Compression Strain**	**Damage Parameter**	**Tension Strain**
0	0	0	0
0.7	0.009	0.7	0.0005

***** Assumed values

Table 6. Steel material property definition input for column model.

Material Property	**Parameter**	**1D2**
Density	Mass Density	7850 kg/m^3 *

***** Assumed values

Table 7. Steel material behavior definition input for column model

Material behavior	**Type**	**Parameter**	**1D2**
Elastic	Isotropic	Young's Modulus	200 GPa *
		Poisson's Ratio	0.3
Plastic	Hardening:		
	Yield Stress / Ultimate Strength	Long. Steel bar	454/ 604 MPa
		stirrups	469/685 MPa

***** Assumed values

Table 8. Parameters used in the parametric study

Cross-section of column (a*b) (mm)	Axial compression index (P_{index})	ρ / $f_y = 454$ (MPa)	ρ_s / $f_y = 469$ (MPa)	f'_c (MPa)	Aspect Ratio (L/d)
350 x 350	0.1	1%*	0.0041	25.8*	5.14*
	0.2*	2%	0.0061*	38	3.5
	0.4	3.2%	0.0123	50	2.8

* As experimental parameters

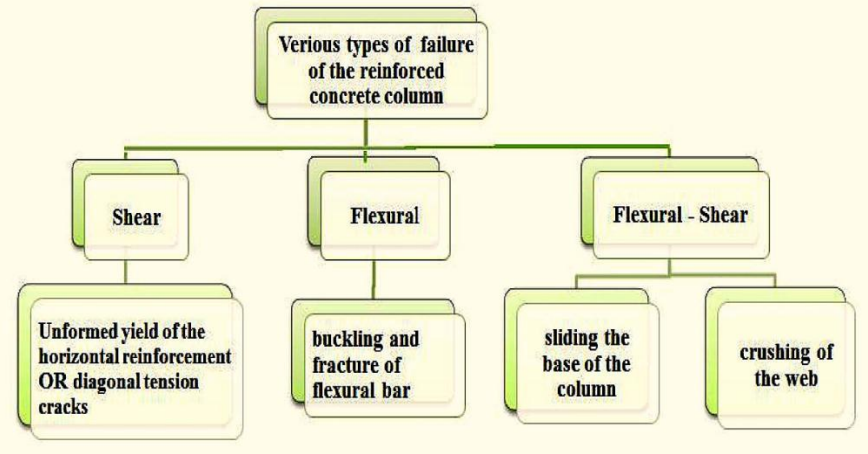

Figure 1. Various types of failure and expected damage of RC columns, Adolfo M., 2006.

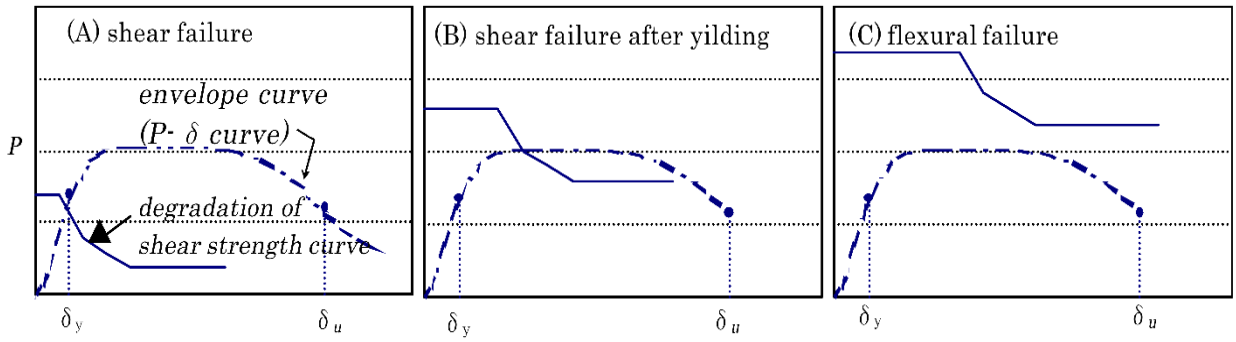

Figure 2. Classification of failure modes of single reinforced concrete column**,** Yoshikawa H., and Miyagi T., 2001.

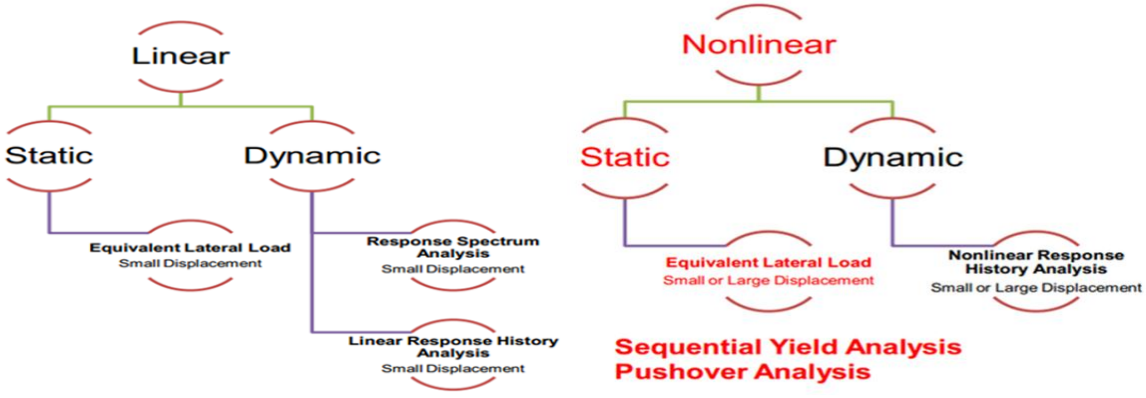

(A) Linear analysis procedures (B) Nonlinear analysis procedures

Figure 3. Analysis procedures, Yoshikawa H., and Miyagi T., 2001.

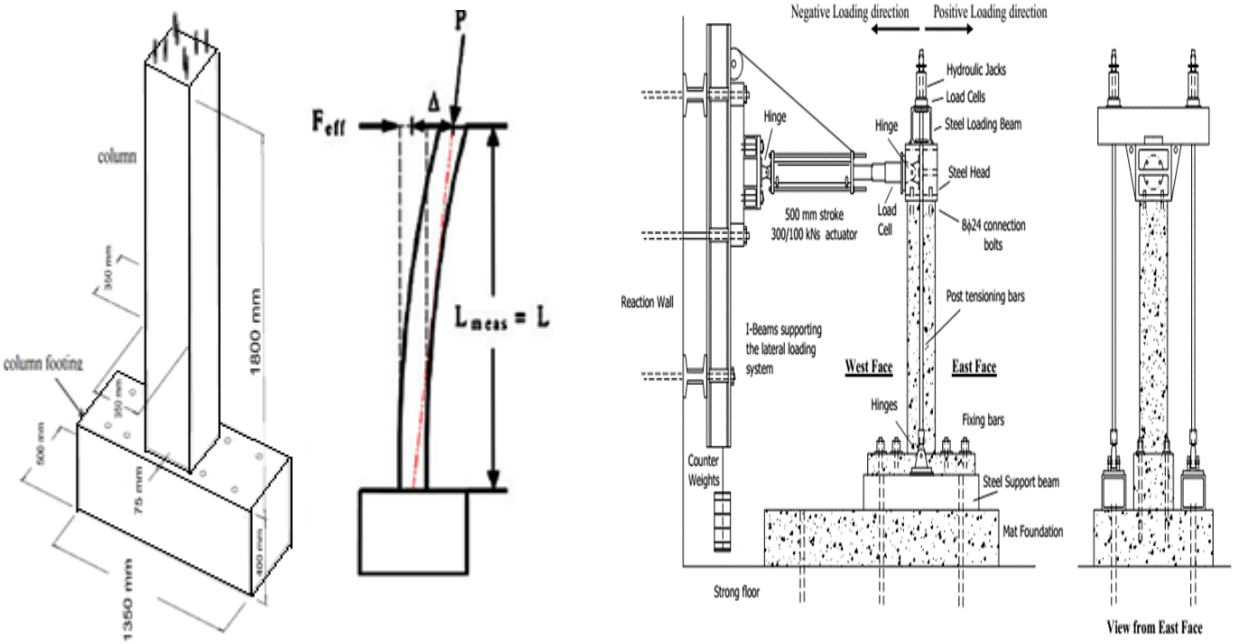

Typical reinforced concrete column specimen Schematic view of test setup

Figure 4. Tested column specimen and set-up, Acun, 2010.

Cycle No	Top Displacement Amp. (mm)	1D2
1		35
2		35
3		35
4		35
5		35
6		35
7		35
8		70
9		70
10		70
11		70
12		70
13		105
14		105
15		105
16		
17		
18		

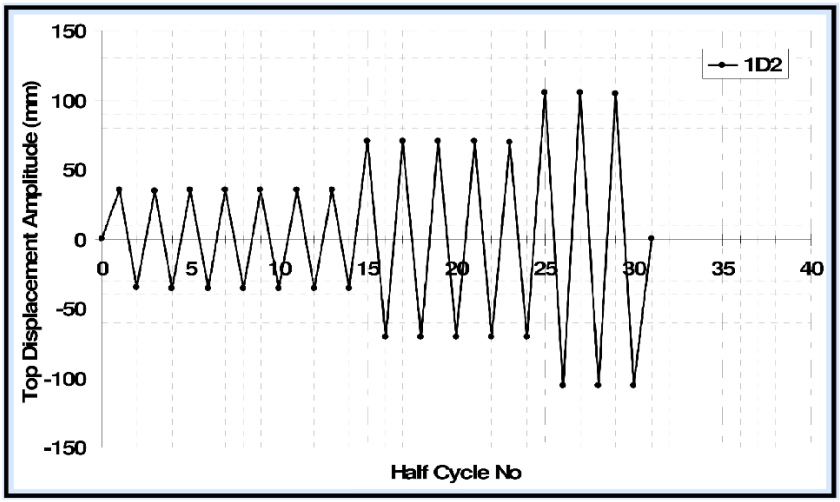

Figure 5. Displacement-time history imposed on the free end of the test specimen, Acun, 2010

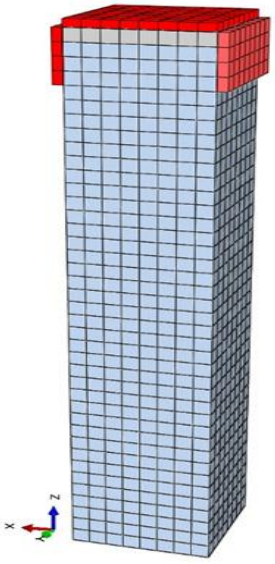

Figure 6. Three dimensional column model adopted in ABAQUS

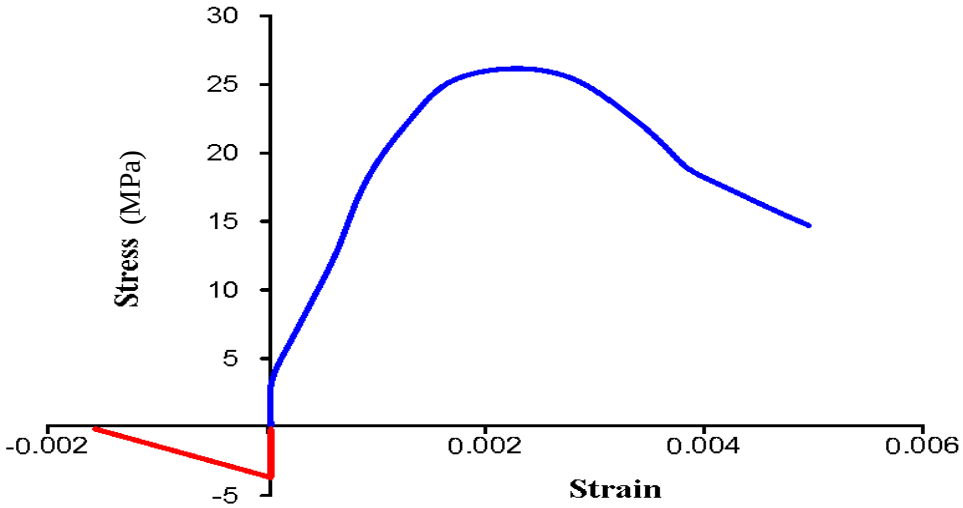

Figure 7. Stress-strain curve for concrete used in ABAQUS model**.**

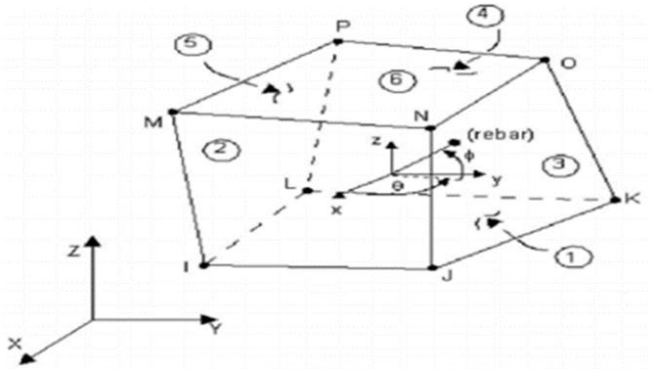

Figure 8. General view of the brick element (C3D8R), **ABAQUS, 2010.**

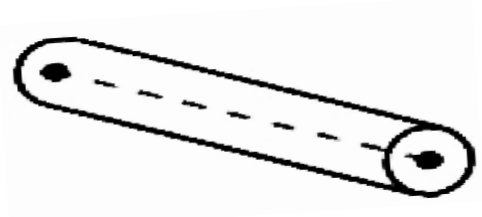

Figure 9. General view of the Truss element (T3D2), **ABAQUS, 2010.**

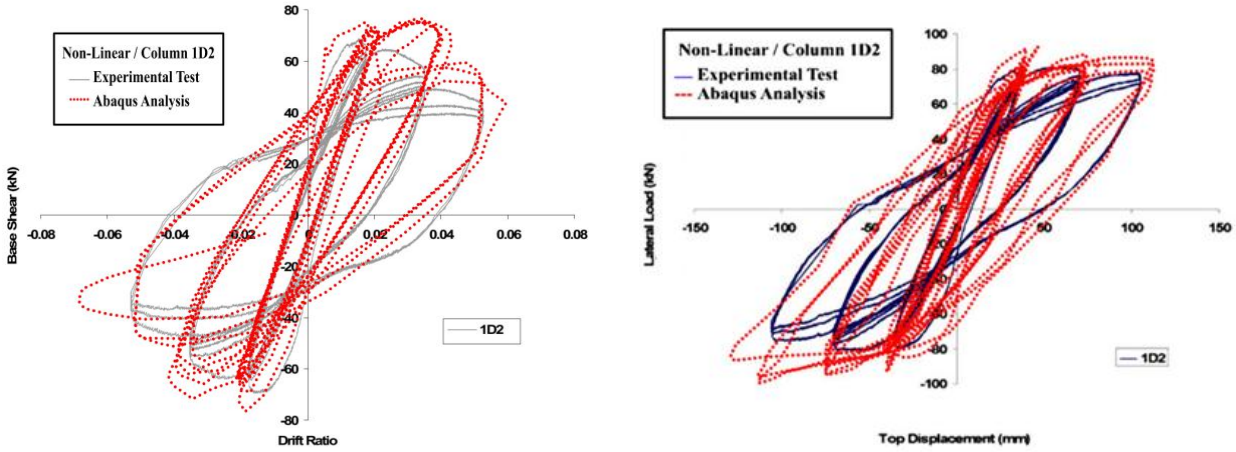

(A) Base shear-drift ratios relation (B) Lateral load-top displacement relation

Figure 10. Analytical and Experimental cyclic responses of the column specimen.

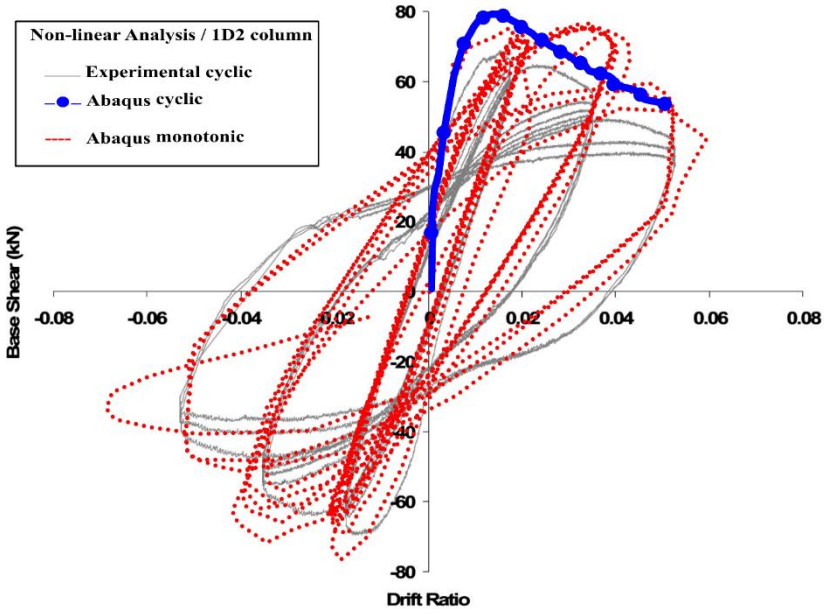

Figure 11. Monotonic and cyclic pushover analysis for the column specimen.

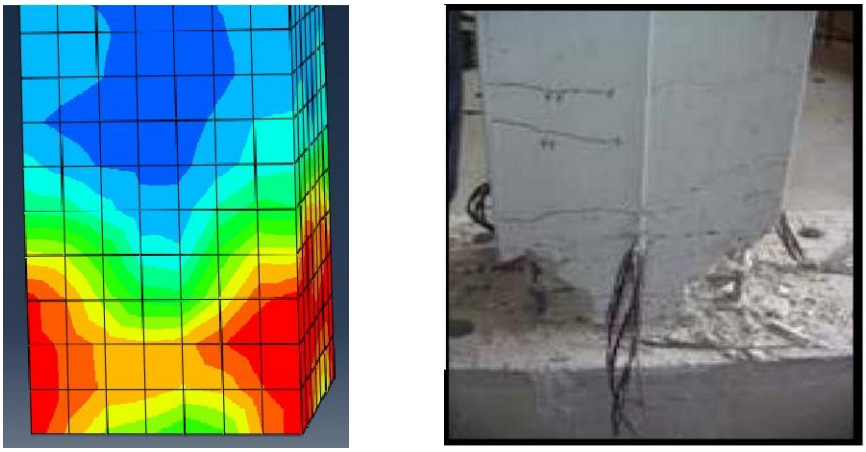

Analytical (present study) Experimental (Acun, 2010)

Figure 12. Comparison between analysis and testing stress distribution at the column base .

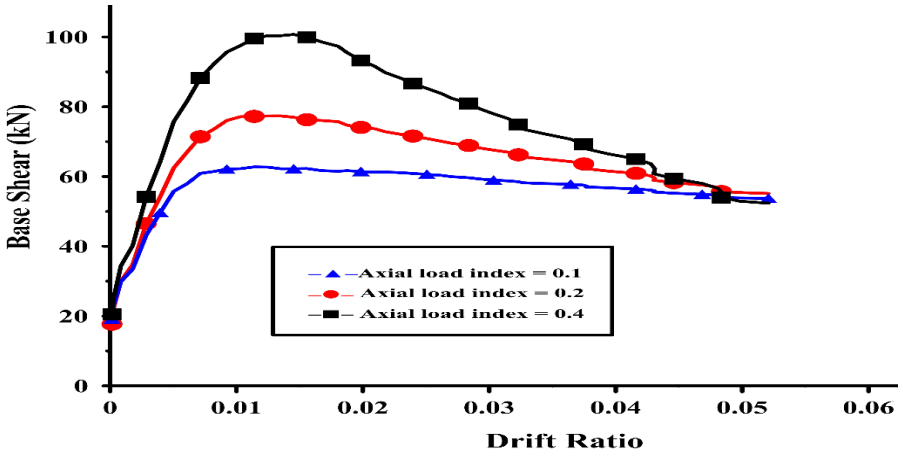

Figure 13. Effect of axial load index on lateral load capacity response.

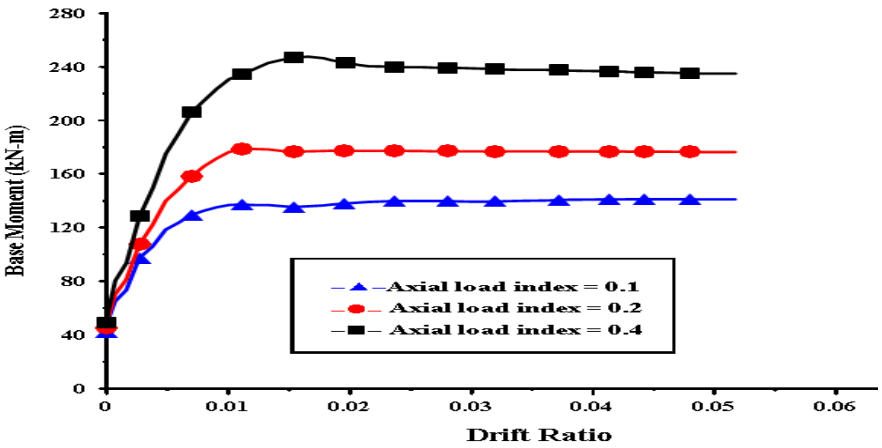

Figure 14. Effect of axial load index on moment capacity response.

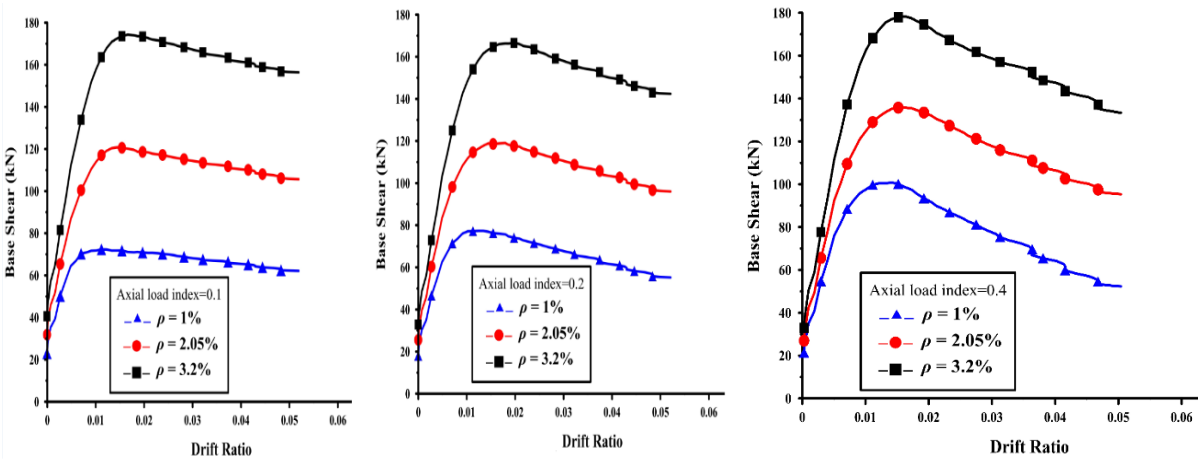

Figure 15. Effect of longitudinal reinforcement ratio on lateral load capacity response for different axial load indices.

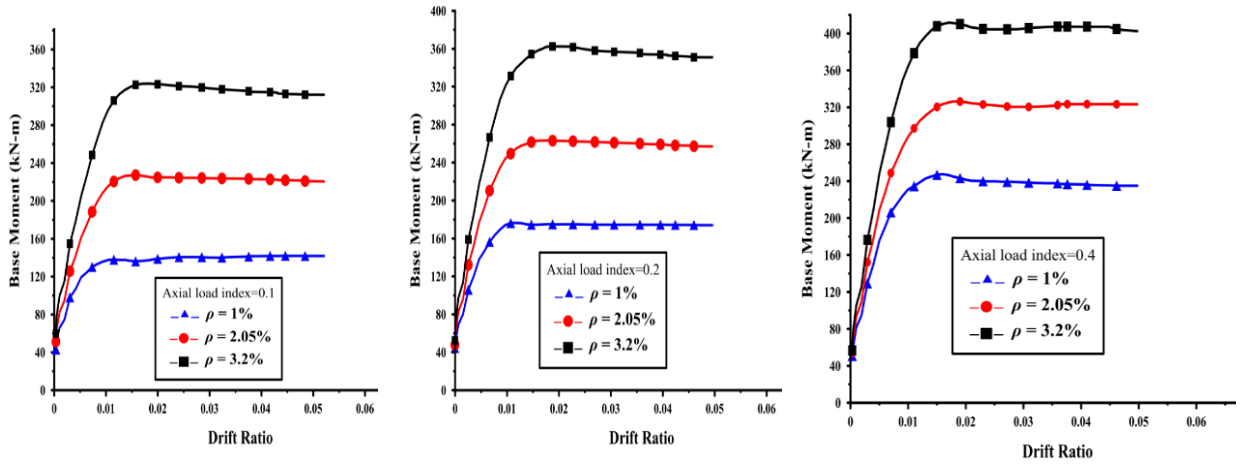

Figure 16. Effect of longitudinal reinforcement ratio on moment capacity response for different axial load indices.

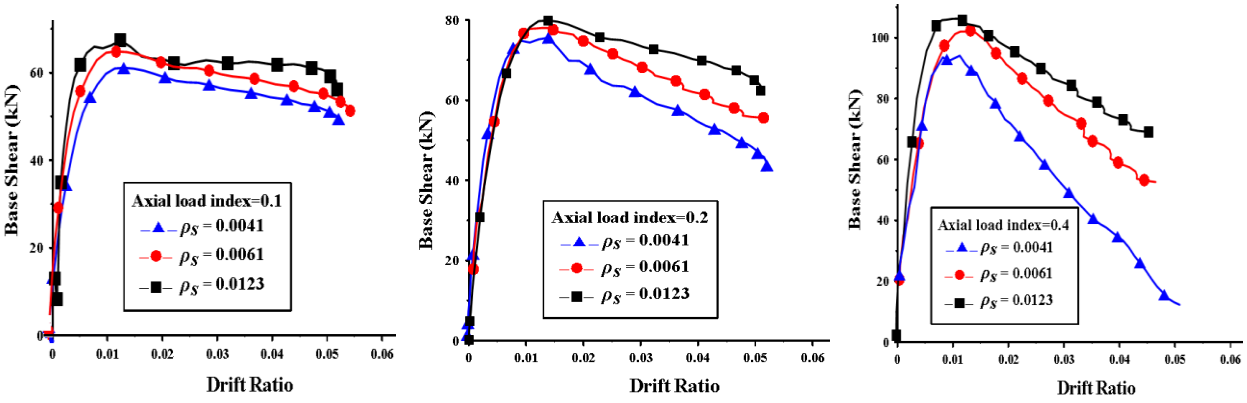

Figure 17. Effect of transverse reinforcement ratio on lateral load capacity response for different axial load indices.

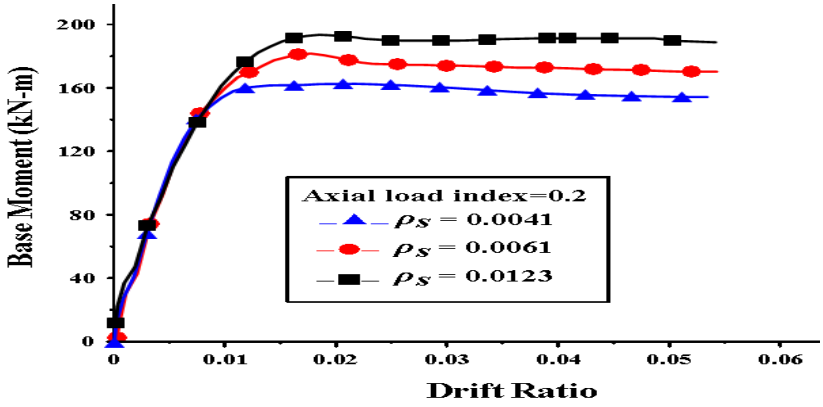

Figure 18. Effect of transverse reinforcement ratio on moment capacity response (Axial load index is 0.2).

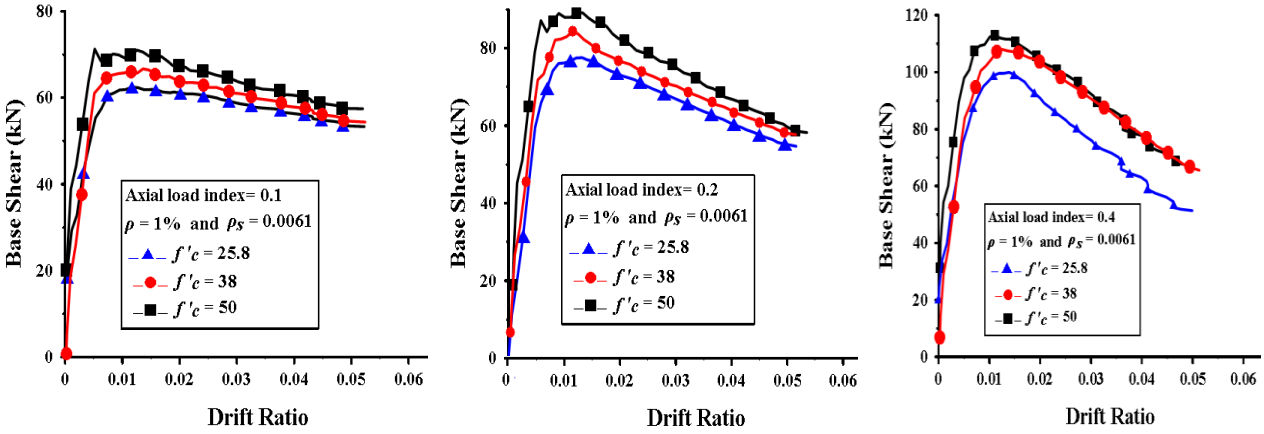

Figure 19. Effect of concrete compressive strength on lateral load capacity response for different axial load indices.

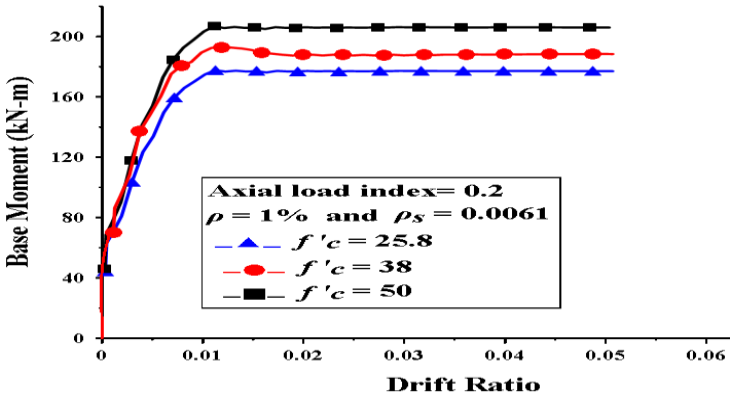

Figure 20. Effect of concrete compressive strength on moment capacity response (Axial load index is 0.2).

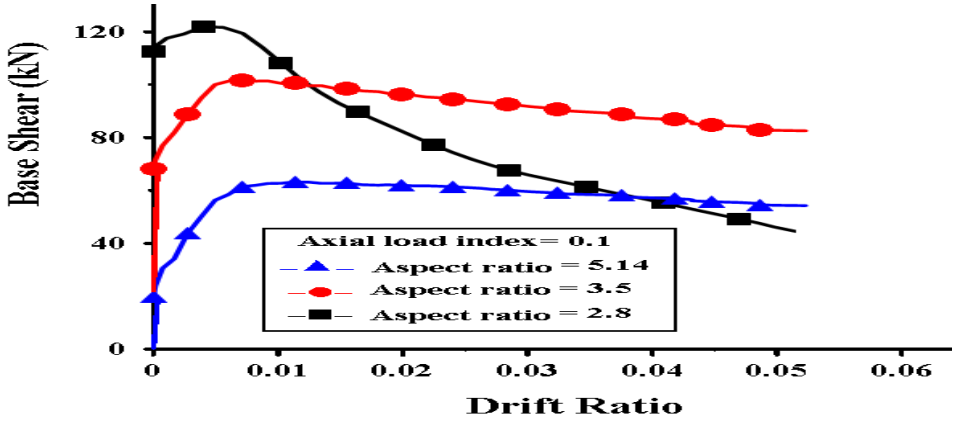

Axial load index is 0.1

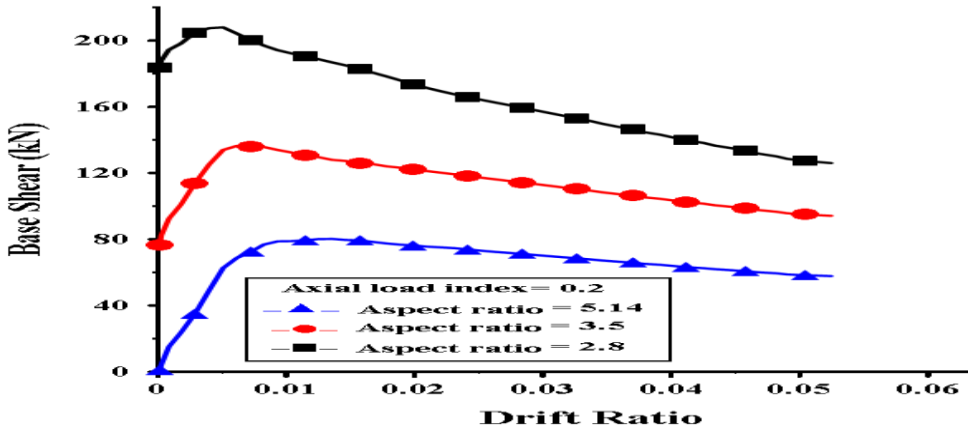

Axial load index is 0.2

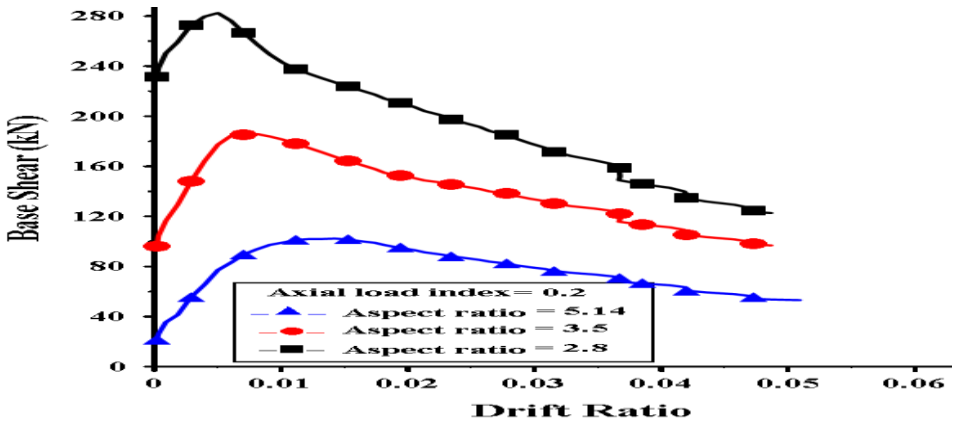

Axial load index is 0.4

Figure 21. Effect of column aspect ratio on lateral load capacity response.